LOCALIZATION OF BURIED SPHERICAL SHELLS BASED ON WIDEBAND SIGNALS

Zineb Saidi

IRENav (EA 3634), Ecole Navale
Lanvéoc Poulmic, BP600
29240 Brest−Armées, France
saidi@ecole-navale.fr

Salah Bourennane

Institut Fresnel, UMR CNRS 6133-EGIM
D.U. de saint Jérome
13 397 Marseille Cedex 20,France
salah.bourennane@egim-mrs.fr

ABSTRACT

This study deals with detection and localization of buried objects. We developed a novel method, that extends the subspace method, to estimate the bearing and the range of buried objects with known shapes such as spheres or cylinders. The idea is to use the spatial complexities of the scattered field to form an acoustic model that we used instead of the plane wave model used in the subspace method. The received signals are wideband and correlated, thus we apply a frequential smoothing in order to decorrelate them. We applied this method first, on cylindrical shells and we obtained a satisfying result [1] and here we will extend it to spherical shells. Performances of the proposed method are investigated on experimental data recorded during underwater acoustic experiments.

1. INTRODUCTION

Acoustic detection and localization of buried objects, in the underwater acoustics environment, has received a great deal of attention, in fact, several methods were developed for mine field remediation, pipeline localization and archaeological site characterization. Some of them use acoustic scattering to localize objects by analyzing acoustic resonance in the time-frequency domain, but these processes are usually limited to simple shaped objects [2]. Other methods using a low frequency synthetic aperture sonar (SAS) have been recently applied on partly and shallowly buried cylinders in a sandy seabed [3]. The major difficulty encountered with the SAS relates to expected large platform movements. This original approach based on the subspace method, such as the MUSIC method [4], has been recently extended to buried objects in the electromagnetic domain [5].
The purpose of our study, is to extend the subspace method to buried objects in the underwater acoustic environment in order to estimate both the range and the bearing of spherical shells. To our knowledge, this is the first time this method has been extended to the underwater acoustic domain, in the presence of correlated wideband signals and without any constraint from a nearfield or farfield region of the array. Our method consists in using an acoustic model [6], associated to spherical shells, at different frequencies, instead of using the plane wave model in the subspace method which estimates only the bearing of objects in the farfield region of the array [4]. Furthermore, the frequencial smoothing (wideband signals) is used in order to decorrelate the signals by means of an average of the focused spectral matrices [7]. Throughout the paper, lowercase boldface letters represent vectors, uppercase boldface letters represent matrices, and lower and uppercase letters represent scalars. The symbol "T" is used for transpose operation and the superscript "+" is used to denote complex conjugate transpose.

2. PROBLEM FORMULATION

We consider a linear array of N sensors which received the wideband signals scattered from P objects ($N > P$) in the presence of an additive Gaussian noise. The received signal vector, in the frequency domain, is given by

$$\mathbf{r}(f_n, \theta, \rho) = \mathbf{A}(f_n, \theta, \rho)\mathbf{s}(f_n) + \mathbf{b}(f_n), \qquad (1)$$

where, $n = 1, ..., L$, $\mathbf{r}(f_n, \theta, \rho)$ is the Fourier transforms of the array output vector, $\mathbf{s}(f_n)$ is the vector of object signals, $\mathbf{b}(f_n)$ is the vector of white Gaussian noise of variance $\sigma^2(f_n)$ and $\mathbf{A}(f_n, \theta, \rho)$ is the transfer matrix (propagation matrix) given by

$$\mathbf{A}(f_n, \theta, \rho) = [\mathbf{a}(f_n, \theta_1, \rho_1), ..., \mathbf{a}(f_n, \theta_P, \rho_P)], \qquad (2)$$

where,

$$\mathbf{a}(f_n, \theta_k, \rho_k) = [a(f_n, \theta_{k1}, \rho_{k1}), ..., a(f_n, \theta_{kN}, \rho_{kN})], \qquad (3)$$

where $k = 1, ..., P$, θ_k and ρ_k are the bearing and the range of the k^{th} object to the first sensor of the array R_1 (see **Fig. 1**), thus, $\theta_k = \theta_{k1}$ and $\rho_k = \rho_{k1}$. The subspace method is based on singular value decomposition of the spectral matrix $\mathbf{\Gamma}(f_n, \theta, \rho)$, in order to separate the object subspace and the noise subspace, which is given by

$$\mathbf{\Gamma}(f_n, \theta, \rho) = \mathbf{A}(f_n, \theta, \rho)\mathbf{\Gamma_s}(f_n)\mathbf{A}^{+}(f_n, \theta, \rho) + \sigma^2(f_n)\mathbf{I}, \qquad (4)$$

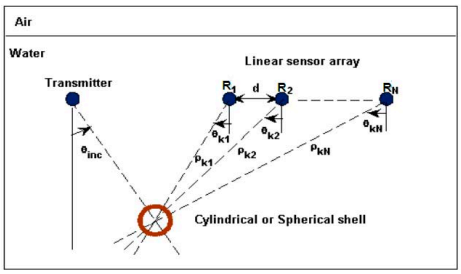

Fig. 1. Geometry configuration of the k^{th} object localization.

where, $\mathbf{\Gamma_s}(f_n)$ is the spectral matrix associated to the object signals and $\mathbf{I}$ is the identity matrix.

3. PROPOSED METHOD

3.1. Acoustic model

In this section we present how to fill the propagation vector used in Eq. (3) at a fixed frequency f_n. Thus, consider the case in which a plane wave is incident, with an angle θ_{inc}, on the object k (infinite cylindrical shell or spherical shell), located in a free space at the bearing θ_k and the range ρ_k). The fluid outside the shells is labeled by 1, thus, the sound velocity c_1 and the wavenumber $K_{n1} = \frac{2\pi f_n}{c_1}$.

Cylindrical shell: as defined in [1], the exact solution of the acoustic scattered field is given by

$$a_{cyl}(f_n, \theta_{k1}, \rho_{k1}) = p_{c0} \sum_{m=0}^{\infty} j^m \epsilon_m b_m H_m^{(1)}(K_{n1}\rho_{k1}) \cos(m(\theta_{k1} - \theta_{inc})), \quad (5)$$

where p_{c0} is a constant, $\epsilon_0 = 1, \epsilon_1 = \epsilon_2 = ... = 2$, b_m is a coefficient depending on limits conditions and m is the number of modes, J_m and N_m represent the Bessel functions and H_m represents the Hankel function.

Spherical shell: in a similar manner, the exact solution of the acoustic scattered field, in this case, is given by [6],

$$a_{sph}(f_n, \theta_{k1}, \rho_{k1}) = p_{s0} \sum_{m=0}^{\infty} B_m H_m^{(1)}(K_{n1}\rho_{k1}) P_m(\cos(\theta_{k1} - \theta_{inc})), \quad (6)$$

where p_{s0} is a constant and $P_m(\cos(\theta_{k1} - \theta_{inc}))$ is the Legendre polynomials [6].

Eq. (5) and Eq. (6) give the first component of the propagation vector, then, in a similar manner the other components $a_{cyl}(f_n, \theta_{ki}, \rho_{ki})$ and $a_{sph}(f_n, \theta_{ki}, \rho_{ki})$ for $i = 2, ..., N$, associated to the i^{th} sensor, can be formed, where θ_{ki} and ρ_{ki} are calculated using the general Pythagorean theorem applied to the configuration shown in **Fig. 1**.

$$\rho_{ki} = \sqrt{\rho_{ki-1}^2 - d^2 - 2\rho_{ki-1} d \cos(\frac{\pi}{2} + \theta_{ki-1})} \quad (7)$$

$$\theta_{ki} = \cos^{-1}[\frac{d^2 + \rho_{ki}^2 - \rho_{ki-1}^2}{2\rho_{ki-1} d}], \quad (8)$$

where d is the distance between two adjacent sensors. Note that, the main goal of the representations given by Eq. (7) and Eq. (8), is to reduce the number of variables to be determined. Thus only θ_{k1} and ρ_{k1} are estimated by the proposed method.

3.2. Frequential smoothing

In this section, the frequency diversity is employed, thus this choice is made in order to decorrelate the signals. The idea is to use the bilinear focusing operator [7], to transform the narrowband data in each frequency bin into a single reference frequency bin f_0. The object subspace is defined as the column span of the transfer matrix $\mathbf{A}(f_n, \theta, \rho)$. Thus, the object subspaces at different frequency bins are different. The coherent subspace methods combine the different subspaces in the analysis band by the use of the focusing matrices. The focusing matrices $\mathbf{T}(f_0, f_n)$ compensate the variations of the transfer matrix with the frequency. Thus these matrices verify $\mathbf{T}(f_0, f_n)\mathbf{A}(f_n, \theta, \rho) = \mathbf{A}(f_0, \theta, \rho)$, The use of the focusing matrices enable us to coherently average the different focused spectral matrices and then to decorrelate the signals [7]. Here, f_0 is the middle frequency of the spectrum of the received signal and it is chosen as the focusing frequency.

The following is the step-by-step description of the developed method:

1. using an ordinary beamformer to find an initial estimate of θ, ρ and the number of objects P,
2. filling the transfer matrix $\hat{\mathbf{A}}(f_0, \theta, \rho)$, given by Eq. (2) and using the estimated parameters of step 1,
3. estimating the spectral matrix output sensors data $\mathbf{\Gamma}(f_n, \theta, \rho)$ using Eq. (4),
4. calculating objects spectral matrix using:
   $\mathbf{\Gamma}_s(f_n, \theta, \rho) = (\hat{\mathbf{A}}^+(f_n, \theta, \rho)\hat{\mathbf{A}}(f_n, \theta, \rho))^{-1}\hat{\mathbf{A}}^+(f_n, \theta, \rho)$
   $[\mathbf{\Gamma}(f_n, \theta, \rho) - \hat{\sigma}^2(f_n)\mathbf{I}]\hat{\mathbf{A}}(f_n, \theta, \rho)$
   $(\hat{\mathbf{A}}^+(f_n, \theta, \rho)\hat{\mathbf{A}}(f_n, \theta, \rho))^{-1}$,
   where, $\mathbf{I}$ is the identity matrix and $\hat{\sigma}^2(f_n)$ the estimated noise variance that is estimated by :
   $\hat{\sigma}^2(f_n) = \frac{1}{N-P}\sum_{i=P+1}^{N} \lambda_i(f_n)$, where $\lambda_i(f_n)$ is the i^{th} eigenvalue of $\mathbf{\Gamma}(f_n, \theta, \rho)$,
5. calculating the average of the spectral matrices associated to the objects:
   $\mathbf{\Gamma}_s(f_0, \theta, \rho) = \frac{1}{L}\sum_{l=1}^{L} \mathbf{\Gamma}_s(f_n, \theta, \rho)$,
6. calculating $\hat{\mathbf{\Gamma}}(f_0, \theta, \rho) = \hat{\mathbf{A}}(f_0, \theta, \rho)\mathbf{\Gamma}_s(f_0, \theta, \rho)\hat{\mathbf{A}}^+(f_0, \theta, \rho)$ and $\hat{\mathbf{\Gamma}}(f_n, \theta, \rho) = \mathbf{\Gamma}(f_n, \theta, \rho) - \hat{\sigma}^2(f_n)\mathbf{I}$,
7. estimating the bilinear focusing operator:
   $\mathbf{T}(f_0, f_n) = \mathbf{V}(f_0)\mathbf{V}^+(f_n)$, where $\mathbf{V}(f_0)$ and $\mathbf{V}(f_n)$ are

the eigenvector matrices of $\hat{\mathbf{\Gamma}}(f_0,\theta,\rho)$ and $\hat{\mathbf{\Gamma}}(f_n,\theta,\rho)$, respectively,

8. calculating the average of the focused matrices: $\bar{\mathbf{\Gamma}}(f_0,\theta,\rho) = \frac{1}{L}\sum_{l=1}^{L}\mathbf{T}(f_0,f_n)\hat{\mathbf{\Gamma}}(f_n,\theta,\rho)\mathbf{T}^{+}(f_0,f_n)$.

Finally, the spatial spectrum is given by $Z(f_0,\theta_k,\rho_k) = \frac{1}{\mathbf{a}(f_0,\theta_k,\rho_k)^{+}\bar{\mathbf{V}}_{\mathbf{b}}(f_0)\bar{\mathbf{V}}_{\mathbf{b}}^{+}(f_0)\mathbf{a}(f_0,\theta_k,\rho_k)}$, where $\bar{\mathbf{V}}_{\mathbf{b}}(f_0)$ is the eigenvector matrix of $\bar{\mathbf{\Gamma}}(f_0,\theta,\rho)$ associated to the smallest eigenvalues.

4. EXPERIMENTAL SETUP

Underwater acoustic data have been recorded in an experimental water tank (**Fig. 2**) in order to evaluate the performances of the developed method. This tank is filled with water and homogeneous fine sand, where are buried four couples of different objects, between 0 and 0.005 m under the sand. The considered objects have the following characteristics:

- the 1^{st} couple: spherical shells, $\emptyset_a = 0.3$ m, $\delta = 0.33$ m, full of air,
- the 2^{nd} couple: cylindrical shells, $\emptyset_a = 0.01$ m, $\delta = 0.13$ m, full of air,
- the 3^{rd} couple: cylindrical shells, $\emptyset_a = 0.018$ m, $\delta = 0.16$ m, full of water,
- the 4^{th} couple: cylindrical shells, $\emptyset_a = 0.02$ m, $\delta = 0.06$ m, full of air,

where δ represents the distance between the two objects of the same couple and $\emptyset_a$ the outer radius (the inner radius $\emptyset_b = \emptyset_a - 0.001$ m).
The considered sand has geoacoustic characteristics close to those of water. Consequently, we can make the assumption that the objects are in a free space. The considered

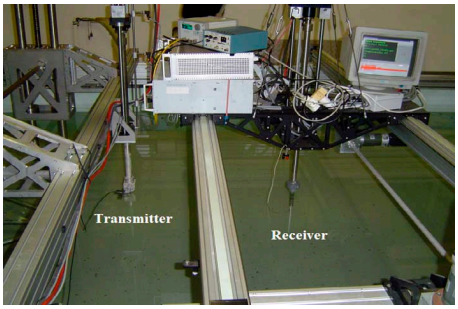

Fig. 2. Experimental tank

objects are made of dural aluminum with density $D_2 = 1800$ kg/m^3, the longitudinal and transverse-elastic wave velocities inside the shell medium are $c_l = 6300$ m/s and $c_t = 3200$ m/s, respectively. The external fluid is water with density $D_1 = 1000$ kg/m^3 and the the internal fluid is water or air with density $D_{3air} = 1.2\ 10^{-6}$ kg/m^3 or $D_{3water} = 1000$ kg/m^3. We carried out eight experiments where the horizontal axis of the transmitter is fixed at 0.45 m from the bottom of the tank with an incident angle $\theta_{inc} = 60^\circ$ and the receiver moves horizontally, step by step, with a step size $d = 0.002$ m and takes 10 positions in order to form an array of sensors with $N = 10$. The first time, we fixed the receiver horizontal axis at 0.2 m from the bottom of the tank, then, we did four experiments, Exp. 1, Exp. 2, Exp. 3 and Exp. 4, associated, respectively, to the 1^{st}, 2^{nd}, 3^{rd} and 4^{th} couple. Then, the horizontal axis of the receiver was fixed at 0.4 m and in the same manner we did four other experiments Exp. 5, Exp. 6, Exp. 7 and Exp. 8 associated, respectively, to the 1^{st}, 2^{nd}, 3^{rd} and 4^{th} couple. For each experiment, the transmitted signal had the following properties; impulse duration is 15 μs, the frequency band is $[f_L = 150, f_U = 250]$ kHz, the mid-band frequency is $f_0 = 200$ kHz and the sampling rate is 2 MHz. The duration of the received signal was 700 μs.

At each sensor, time-domain data was collected and the

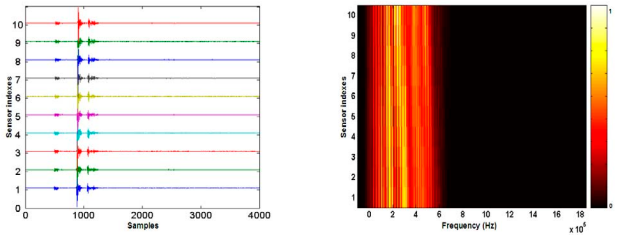

(a) (b)

Fig. 3. Experimental data. (a) Time. (b) Frequency.

sensor output signals associated to one experiment are shown in **Fig. 3**.

5. EXPERIMENTAL RESULTS

The steps listed above in section 3.2, are applied to each experimental data, thus, we did an initialization of θ, ρ and P using the conventional beamformer and for example for Exp. 1, those three parameters had been initialized by $P = 1$, $\theta_1 = 15^\circ$ and $\rho_1 = 0.28$ m. Furthermore, the average of the focused matrices was calculated using $L = 50$ frequencies and a sweeping on the bearing and the range had been applied ($[-90^\circ, 90^\circ]$ for the bearing with a step 0.1° and $[0.15, 0.7]$ m for the range with a step 0.002 m). The obtained spatial spectrum of the proposed method associated to the spherical shells and some of those associated to the cylindrical shells that had been presented in [1], are shown in **Fig. 4**.

Table 1 summarizes the expected and the estimated range

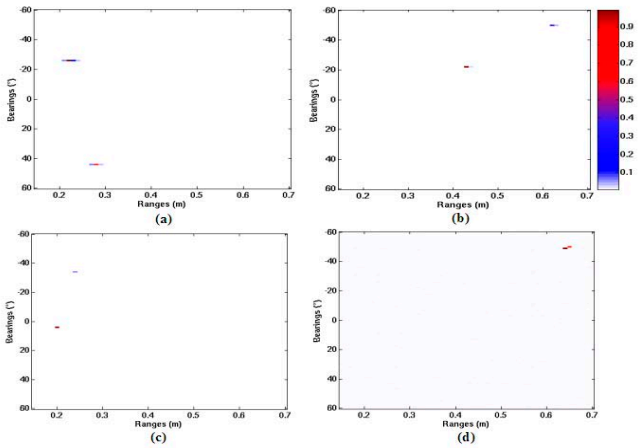

Fig. 4. Spatial spectrum of the proposed method. (a) Exp.1. (b) Exp.5. (c) Exp.3. (d) Exp.8

and bearing objects obtained using the proposed method. The indexes 1 and 2 are the 1^{st} and the 2^{nd} object of the same couple. Satisfying results are obtained, thus the majority of bearing and range objects are successfully estimated. Furthermore, the difference between the estimated values $\theta_{(1,2)est}$, $\rho_{(1,2)est}$ and the expected values $\theta_{(1,2)exp}$, $\rho_{(1,2)exp}$ is very small. Thus, we obtained an $\mathrm{RMSE}_\theta = 0.48^\circ$ and $\mathrm{RMSE}_\rho = 0.02$ m using the following equation $\mathrm{RMSE_X} = \sqrt{\frac{\sum_{i=1}^{8}\left[(\mathrm{X_{exp1}}-\mathrm{X_{est1}})_i^2+(\mathrm{X_{exp2}}-\mathrm{X_{est2}})_i^2\right]}{16}}$, where X represents θ or ρ and i the experiment. One cylinder was not localized in Exp. 6, because, the received echo, associated to this cylinder, is rather weak, thus, it is important to realize that there are some phenomena which complicate the object detection in an experimental tank, as the attenuation of high frequencies in sediment is much higher than low frequencies. The frequencies used here are $[150, 250]$ kHz represent high frequencies.

6. CONCLUSION

In this study, we have proposed a novel method to estimate both the range and the bearing of buried objects. An acoustic model, developed using the exact solution of the scattered field, is used, therefore, there are no constraints from nearfield or farfield region of the array. Furthermore, we have taken into account the correlated signal problem and to cope with this problem, we used the bilinear focusing operator. Therefore, the objects can be localizes even if the received signals are totally correlated. The performances of this method are investigated through experimental data associated to many spherical and cylindrical shells buried under the sand. The proposed method is superior in terms of performance to the conventional method.

	Exp.1	Exp.2	Exp.3	Exp.4
$\theta_{1exp}(^\circ)$	-26.5	-23	-33.5	-32.5
ρ_{1exp}(m)	0.24	0.24	0.26	0.26
$\theta_{2exp}(^\circ)$	44	9.2	5.5	-20
ρ_{2exp}(m)	0.31	0.22	0.24	0.22
$\theta_{1est}(^\circ)$	-25	-23	-33	-32
ρ_{1est}(m)	0.22	0.25	0.26	0.28
$\theta_{2est}(^\circ)$	43	9	6	-20
ρ_{2est}(m)	0.32	0.24	0.25	0.23
	Exp.5	Exp.6	Exp.7	Exp.8
$\theta_{1exp}(^\circ)$	-50	-52.1	-50	-51.6
ρ_{1exp}(m)	0.65	0.65	1.24	0.65
$\theta_{2exp}(^\circ)$	-22	-41	-42.5	-49.5
ρ_{2exp}(m)	0.45	0.56	0.58	0.64
$\theta_{1est}(^\circ)$	-49	$-$	-50	-51
ρ_{1est}(m)	0.65	$-$	0.64	0.63
$\theta_{2est}(^\circ)$	-22	-41	-42	-49
ρ_{2est}(m)	0.44	0.55	0.57	0.62

Table 1. The obtained range and bearing objects. ($-\theta$ is clockwise from the vertical)

7. REFERENCES

[1] Z.Saidi and S.Bourennane, "Buried objects localization in presence of correlated signals," *IEEE Workshop Statistical Signal Processing*, Bordeaux, France 2005.

[2] G. Nicq and M. Brussieux, "A time-frequency method for classifying objects at low frequencies," *Proc. OCEANS'98*, vol. 1, 1998.

[3] B. Zerr M. Legris R. Bellec J. C. Sabel A. Hetet, M. Amate and J. Groen, "Sas processing results sor the detection of buried objects with a ship-mounted sonar," *Proc. of the 7th Conf. on Underwater Acoustics*, July 2004.

[4] R. O. Schmidt, "Multiple emitter location and signal parameter estimation," *IEEE Trans. Antennas Propagat.*, vol. AP-34.

[5] A. Sahin and E. L. Miller, "object-based localization of buried objects using high resolution array precessing techniques," *Proc. of the SPIE Int. Conf. - AeroSense*, vol. 2765, may 1996.

[6] W. L. J. Fox J. A. Fawcett and A. Maguer, "Modeling by scattering by objects on the seabed," *J. Acoust. Soc. Am.*, vol. 104, no. 6, December 1998.

[7] S. Valaee and P. Kabal, "wideband array processing using a two-sided correlation transformation," *IEEE trans. on Signal Processing*, vol. 43, no. 1, 1995.